Infrared Evidence for the α-Helical-type Structure of Very Simple N-Octanoyl-L-glutamic Acid Oligomers (Residue Number, N = 1–4) and for the α-CO$_2^-$ Group Effect on their $\alpha \to \beta$-like Transition

Toshiyuki Uehara, Hirofumi Okabayashi,* Keijiro Taga and Tadayoshi Yoshida
Department of Applied Chemistry, Nagoya Institute of Technology, Gokiso-cho, Showa-ku, Nagoya 466, Japan

Hiroshi Kojima
Gifu National College of Technology, Shinsei-cho, Motosu-gun, Gifu, 501-04, Japan

Very simple N-octanoyl-L-glutamic acid oligomers (residue number, N = 1–4) have been synthesized and the vibrational spectra of these oligomer films, made by casting them from a dimethylformamide solution onto an NaCl plate, have been investigated together with their time dependence. The results have been compared with those of two β-forms (β_1 and β_2) and the α-helix of the longer N-octanoyl-L-glutamic acid oligomers (N = 6–14) and with those of poly(L-glutamic acid). Even the N-octanoyl monomer and the dimer as well as the trimer and the tetramer take up an α-helical-type structure, in which the hydrogen-bonding network formed by the α,γ-CO$_2$H and the peptide groups are very similar to that in α-helical poly(L-glutamic acid). For the cast films of these simple oligomers, a transition similar to the $\alpha \to \beta_1$ or $\alpha \to \beta_2$ transition in poly(L-glutamic acid) is observed at 20 °C. In particular, ionization of the α-CO$_2$H groups in the cast films is promoted at a higher relative humidity. The $\alpha \to \beta$-like transition is promoted by the α-CO$_2^-$ group so formed.

In proteins, most α-helical structures are very short and have a range of 6–20 residues.[1] Charged groups play a critical role in the formation of such short α-helices. Bierzynski *et al.*[2] found that the stability of the α-helix of the isolated C-terminal peptide (residues 1–13) of ribonuclease A is strongly pH-dependent within the pH range 2–8. Kim and Baldwin[3] showed that deprotonation of the CO$_2$H terminus destabilizes the helical structure. Furthermore, the helix-forming properties of chemically synthesized C-terminal peptide analogues have been investigated in detail by Shoemaker *et al.*[4] The results indicate that the charged-group effect on the stability of the C-terminal peptide helix can be explained by so-called 'α-helix dipole model'.[5]

The charged-group effect has also been observed for very simple homo-oligopeptides. For N-acylglycine oligomers (N = 3–5),[6,7] it has been elucidated by vibrational spectroscopy and X-ray powder pattern methods that a deprotonated CO$_2$H terminus stabilizes the polyglycine II-like helical structure. However, for the case of N-acyl-L-alanine oligomers (N = 3, 4), we have found that introduction of a terminal α-CO$_2^-$ group does not bring about stabilization of the α-helical structure.[8] These observations reveal that a terminal α-CO$_2^-$ group effect may be dependent on the nature of the residues in the oligopeptide. Accordingly, it was deemed advisable to investigate further their charged-group effect on the conformation of simple homo-oligopeptides having a variety of residues.

In our previous paper,[9] X-ray powder diffraction patterns and vibrational spectra provided ample evidence that the octanoyl oligomers (N = 8–22) take up both β_1- and β_2-type structures and that the oligomer films cast onto NaCl or KBr plates take up an α-helical structure. Furthermore, it has been revealed that preferential stabilization of the β_1- or β_2-forms and the $\alpha \to \beta_1$ or $\alpha \to \beta_2$ transition is strongly dependent on the number of residues in the oligopeptide.

In this investigation such an $\alpha \to \beta$-like transition has been investigated in detail for very short N-octanoyl oligomers (N = 1–4) by use of vibrational spectra, in order to understand the role of a terminal α-CO$_2^-$ group in such a conformational change. The kinetics of the transition for these very

short octanoyl oligomers is not discussed herein but will be reported separately. The present discussion is focussed on the IR spectral evidence for the origin of further destabilization of an α-helical-type structure for the cast films of these oligomers at high relative humidity.

Itoh *et al.*[10] have reported that formation of two β-forms (β_1 and β_2) is induced by heating of α-helical poly(L-glutamic acid) [α-poly(Glu)]. Heating of α-poly(Glu) from 313 to 358 K results in β_1 formation, and raising the temperature above 358 K causes the $\beta_1 \to \beta_2$ transition. Analysis of X-ray powder patterns[10–12] for two modifications of β-poly(Glu) shows that the intersheet distances are 8.8–9.03 Å for β_1 and 7.8–7.83 Å for β_2 and that the pleated sheets of the β_2 form are more tightly packed than are those of the β_1-form.

In this paper infrared absorption bands[10,13,14] characteristic of the secondary structures (α-, β_1- and β_2-forms) of poly(Glu) are used as references for interpretation of the infrared absorption spectra of the short octanoyl oligomers. In particular, the amide A, I, II and V modes[15–22] characteristic of the secondary structure of polypeptides are used for the detailed discussion of the conformations of the octanoyl oligomers.

Experimental

Materials

N-Octanoyl-L-glutamic acid oligopeptides [octanoyl oligomers, CH$_3$(CH$_2$)$_6$CO(NHCH(CH$_2$CH$_2$CO$_2$H)CO)$_N$OH, N = 1–4] were synthesized by a stepwise procedure described previously.[9] The compounds were dissolved in dimethylformamide (DMF) and dried diethyl ether was added to the solution until a precipitate appeared. The precipitate was then collected by filtration and dried under high vacuum at room temperature (*ca.* 25 °C). These oligomers were identified by elemental analysis.

N-Octanoyl-L-glutamic acid oligomers (N = 1–3) were dissolved in methanol–water and the pH of the solution was adjusted to 7.0 by slowly adding dilute NaOH–H$_2$O at 0 °C. The sodium salts of these oligomers were collected by lyophi-

lization and dried under high vacuum at room temperature over P_2O_5.

A drop of the sample–DMF solution was cast onto an NaCl plate, and the DMF solvent was removed by evaporation in vacuo. This treatment provided transparent cast films of all the short octanoyl oligomers.

Methods

Infrared spectra were recorded on a Perkin–Elmer 1600 FTIR spectrometer (4000–600) cm^{-1}. Films cast onto an NaCl plate were used for the $\alpha \rightarrow \beta$-like transition experiment. All FTIR measurements for these cast films were made at 20 °C and at two relative humidities (60 and 70%). The resolution of the measurements was 4 cm^{-1}. The number of accumulations per spectrum was 64 for the α-type cast films and 10 for each $\alpha \rightarrow \beta$-like transition experiment. The transition was followed by 1 min intervals. X-Ray powder diffraction patterns were obtained by use of an RAD-RC diffractometer with counter-monochromator (Cu-Kα, 60 kV, 200 mA).

Results and Discussion

In our previous paper,[9] the FTIR spectra for the transparent films of the octanoyl oligomer series ($N = 3$–14), which were made by casting them from a DMF solution onto an NaCl plate, were compared with those of the two β-forms (β_1 and β_2) and the α-helix of poly(Glu). These IR spectra were satisfactorily explained in terms of the α-helix.

In the present study, the IR spectral features for the transparent cast films of the octanoyl monomer and dimer are also assigned to either the α-helical or the β_1- or β_2-type structures, and the structure of the cast films and the mechanism of a transition in these films, similar to the $\alpha \rightarrow \beta_2$ transition of poly(Glu), are discussed in detail. For ease of discrimination among the α-helix and the β_1- and β_2-like structures, the characteristic bands of the α-helical, β_1- and β_2-like octanoyl oligomers[9] and poly(Glu)[10,23] are briefly summarized in Tables 1–3.

α-Helical Type Octanoyl Monomer and Dimer Cast Films

Fig. 1 shows the IR spectra of the films for the octanoyl monomer, dimer, trimer and tetramer, cast onto an NaCl plate. The observed band frequencies characteristic of the α-helical structure are listed in Table 1 together with a tentative assignment. On the whole, the IR spectral features of the octanoyl monomer and dimer are very similar to those of the α-helical octanoyl trimer and tetramer. Note that the bands observed at 1387–1392 cm^{-1} (arising from the wagging modes of the side-chain CH_2 groups) and those at 667–671 cm^{-1} (due to the amide V mode) are characteristic of an α-helical structure.[9,10] The 1718–1720 cm^{-1} bands, due to the asymmetric $C=O$ stretching mode of cyclic CO_2H dimers, closely correspond to the 1719–1723 cm^{-1} bands of α-helical octanoyl oligomers ($N = 3$–14)[9] and to the 1718 cm^{-1} band for α-helical poly(Glu).[10] The unperturbed bands at 3264–3277 cm^{-1} are also very close to those of α-helical-type octanoyl oligomers ($N = 3$–14)[9] and that for α-poly(Glu).[10] The OH stretching mode of the CO_2H group is expected in the same region as the NH stretching, but no sharp band is generally observed.

Table 1 Observed infrared absorption band frequencies (cm^{-1})[a] characteristic of α-helical octanoyl oligomers (residue number, $N = 1$–8) in cast films[b]

| octanoyl oligomers (N)[c] | | | | α-helical | | |
1	2	3	4	(6–8)[d]	Poly(Glu)[e]	assignment[e,f]
3290[g] s	3293[g] s	3293[g] s	3294[g] s	3282–3292[g] s	3301[g] vs	amide A
(3264)[h]	(3277)[h]	(3277)[h]	(3282)[h]	(3274–3276)[h]	(3268)[h]	
3065[g] s	3074[g] s	3072[g] s	3076[g] s	3066–3074[g] s	3067[g]	amide B
2956 ms	2956 s	2956 s	2956 s			
2930 vs	2931 vs	2932 vs	2931 vs	2934–2935 ⎱		ν(CH)
2871 w	2871 w	2871 w	2874 w	2876–2877 ⎰		
2859 w	2859 w	2859 w	2860 w			
1720 vs	1718 vs	1718 s	1719 s	1712–1723 s	1718 s	ν[C=O(CO$_2$H)]
1643 vs	1644 vs	1647 vs	1646 vs	1644–1649 vs	1653 vs	amide I
1546 s	1545 s	1544 s	1544 s	1541 s	1550 s	amide II
1453 m	1450 m	1450 sh	1449 sh	1449 sh	1451 w	s(CH$_2$)
1416 m	1415 m	1414 m	1414 m	1415 m	1417 m	
1387 m	1390 m	1392 m	1390 m	1388–1389 m	1388 m	ω(CH$_2$)
		1342 vw	1338 vw	1339–1340 vw	1343 sh	
1290 sh	1290 sh	1295 sh	1295 sh	1291–1294 sh	1283 w	amide III
1252 m	1254 m	1254 m	1254 m	1255–1256 m	1253 ms	ν[C—O(CO$_2$H)]
1214 m	1215 m	1218 m	1214 m	1212–1214 m	1212 m	ω(CH$_2$)
1179 m	1179 m	1179 m	1179 m	1177–1182 m	1181 w	H$^\alpha$bend + t(CH$_2$)
1132 w	1133 w	1130 w	1130 w	1128–1136 w	1118 w	ν(N—C$^\alpha$), ν(C$^\alpha$—C$^\beta$)
1104 w	1106 w	1106 w	1106 w	1105 w	1083 w	ν(C$^\alpha$—C$^\beta$)
1064 vw	1064 vw	1063 vw	1063 vw	1063 vw	1060 w	
932 vw	934 vw	934 vw	934 vw	934–938 vw	928 w	ν(C—N), ν(C$^\alpha$—C)
	898 vw	897 vw	893 vw	894–899 vw	896 w	
865 vw	864 vw	866 vw	864 vw	865 vw	869 w	
810 w	815 w	818 vw	818 vw	810–822 vw	824 mw	r(CH$_2$)
		705 sh	705 sh	703–705 sh	705 w	
671 w	668 w	668 w	667 w	669–670 w	670 mw	amide V

[a] s, strong; m, medium; w, weak; v, very; sh, shoulder. [b] Only the main vibrational bands characteristic of the α-helical type are listed. [c] N is the residue number of octanoyl oligomers. [d] From ref. 9. [e] From ref. 14. [f] Amide A, N—H stretching and amide B, the overtone mode of amide II. [g] Observed frequency. [h] Corrected for Fermi resonance using the equation of $\nu_{\text{amide A}}$(unperturbed) $= \nu_{\text{amide A}}$(perturbed) $- [2(\nu_{\text{amide II}})$ $- \nu_{\text{amide B}}$(perturbed)]. The averaged values of the observed frequencies for amide A, amide B and amide II were used for calculation of these corrected frequencies.

Table 2 Observed IR band frequencies $(cm^{-1})^a$ characteristic of β_2-type octanoyl oligomers $(N = 3, 4, 8\text{–}14)^{b, c}$ and poly(Glu)^c

β_2-type octanoyl oligomers^b							
$N = 3$			$N = 4$		$N = 8\text{–}14$ crystal^c	β_2-type poly(Glu)^c	assignment$^{c, f}$
film^d			film^d				
r.h. 60%	r.h. 70%	crystal^e	r.h. 60%, 70%	crystal^e			
3334^g s	3330^g s	3336^g s	3337^g s	3340^g s	3338–3342^g s		amide A
(3321)^h	(3312)^h	(3322)^h	(3321)^h	(3320)^h	(3339)^h		
3084^g m	3086^g	3088^g m	3086^g m	3089^g m	3090–3100^g m		amide B
2953 m	2955 m	2954 m, sh	2956 m, sh	2957 m, sh	2967–2978 w		
⌠2929 m	2931 m	2933 m	2931 m	2937 m	2942–2945 w		v(CH)
⌡2918 m							
2874 vw	2870 vw	2872 w, sh	2872 w	2873 w			
2852 w	2857 w	2860 w	2858 w	2863 w, sh			
1735 vs	1735 vs	1736 vs	1734 vs	1732 vs	1734–1736 vs	1732 vs	$v[C=O(CO_2H)]$
1640 sh	1635 m, sh	1639 s	1643 s	1640 w			
1620 s	1623 vs	1628 vs					
1604 vs	(1599 m, sh)^i	(1598 m, sh)^i	1609 vs	1602 vs	1606–1610 vs	1601 vs	amide I
1553 s	1552 vs	1551 s	1551 s	1553 s	1543–1552 s	1554 s	amide II
1445 w	1445 w	1444 m	1444 w	1442 w	1443 w	1441 w	
1414 w	1411 m	1414 m	1413 m	1415 m	1413–1415 m ⎱	1417 m ⎱	$s(CH_2)$
				1410 m	1408–1411 m ⎰	1408 m ⎰	
1294 vw	1295 vw	1294 vw	1295 w	1294 w	1294–1295 w	1295 w ⎱	amide III
1271 m	1271 m	1269 m	1274 m	1274 m	1274–1275 m	1280 m ⎰	
1249 m	1240 w		1237–1238 w	1237 w	1237–1238 w	1236w ⎱	
1192 vw	1194 w	1193 vw	1191–1192 w	1191 m	1191–1192 m	1190 m ⎰	$\omega(CH_2)$
1172 m	1171 m	1173 m	1169–1170 m	1168 s	1168–1170 s	1168 s	$t(CH_2)$
1064 vw	1064 w	1063 w	1063–1064 vw	1063 vw	1064 vw	1065 vw	$v(C-N, C-O)$
941 vw	949 w	949 w	947–948 vw	947 vw	950–952 vw	952 vw ⎱	$v(C-C), v(C-O)$
892 vw		901 w	894–895 vw	893 vw	889–890 vw	885 vw ⎰	
						834 vw ⎱	$r(CH_2)$
790 w	792 m	793 m	791–792 m	790 m	791–792 m	789 m ⎰	

^{a} Abbreviations as in Table 1. ^{b} N is the residue number of octanoyl oligomers. ^{c} From ref. 9 and 10. ^{d} Made by casting the octanoyl oligomers from a DMF solution onto a NaCl plate. ^{e} For these octanoyl oligomer samples the X-ray powder diffraction patterns were measured and lattice spacings (7.66–7.81 m, 4.70–4.74 s, 3.91–3.96 vs, 3.57–3.62 m, 3.11–3.18 w, 2.61 w and 2.31–2.34 vw Å) characteristic of β_2-type structure were confirmed. ^{f} v, stretching; s, scissoring; t, twisting; w, wagging; r, rocking; bend, bending vibration; amide I, mainly C=O stretching; amide II, N—H in-plane bending vibration coupled with amide C—N stretching; amide III, mainly amide C—N stretching and amide V, mainly N—H out-of-plane bending vibration. ^{g} Observed frequencies. ^{h} Corrected for Fermi resonance. ^{i} Overlaps with the $v_{as}(\alpha\text{-}CO_2^-)$ band.

For the IR spectra of the α-helical-type simple octanoyl oligomers $(N = 1\text{–}4)$, the bands at 2859–2860, 2871–2874, 2930–2932 and 2956 cm^{-1} are observed in common and are assigned to the CH stretching (v_{CH}) bands arising from glutamic acid residues and N-octanoyl groups. The 2871–2874

Table 3 Observed IR band frequencies $(cm^{-1})^a$ characteristic of β_1-type octanoyl oligomers $(N = 1, 8\text{–}14)^{b, c}$ and poly(Glu)^c

octanoyl monomer cast film	octanoyl oligomers$^{b, c}$ $N = 8\text{–}14$	poly(Glu)^c
1716 vs	1714–1716 vs	1711 vs
1630 s	1631–1638 vs	1625 vs
1554 vs	1535–1541 s	1523 s
1450 m	1444–1448 m	1444 m
1412 m	1409–1414 m	1414 m
1335 w	1334–1339 w	1336 w
1250 w	1257–1260 m	1254 m
1236 w	1218–1232 m	1230 w
1206 m	1208–1218 sh	1208 w
1174 m	1172–1181 m	1175 w
1135 w	1133–1136 w	1137 w
946 vw	945–951 vw	952 vw
932 vw	932–939 vw	932 w
820 vw	819–825 vw	822 w
690 vw	692–702 w	698 w

^{a} s, strong; m, medium; w, weak; v, very; sh, shoulder. ^{b} N is the residue number of octanoyl oligomers. ^{c} From ref. 9 and 10.

cm^{-1} bands are assigned to the v_{CH} modes of glutamic acid residues, since these bands increase in intensity with increasing number of residues. For α-poly(Glu),^{14} the v_{CH} bands were observed at 2880 (s, b) and 2939 (m) cm^{-1}. Therefore, the bands at 2871–2874 and 2930–2932 cm^{-1} for the α-helical-type octanoyl oligomers arise from the v_{CH} mode of both the glutamic acid residues and octanoyl groups. The bands at 2859–2860 cm^{-1} for α-type octanoyl oligomers mainly come from the v_{CH} modes of N-octanoyl groups.

The IR bands for α-helical-type octanoyl oligomers $(N = 1\text{–}4)$ are broader than those of the β_2-type octanoyl oligomers,^{9} implying a smaller degree of crystallinity and lower order in these cast films.

In the very simple α-helical-type octanoyl oligomers, both the α- and γ-CO_2H groups seem to take part in the inter- and intra-molecular hydrogen-bonding network in the cast films, since no bands characteristic of the α- and γ-CO_2^- groups are found (Fig. 1).

The number of residues in the monomer, dimer and trimer is too small for completion of one α-helical turn. However, for α-poly(Glu) the hydrogen-bonding networks, which are formed by the side-chain CO_2H groups, must play a critical role in formation of the α-helical-type structure.^{24} Therefore, for the α-helical-type cast films of very simple octanoyl oligomers, the inter- and intra-molecular hydrogen-bonding networks are probably formed by the α- and γ-CO_2H groups and are very similar to α-helical poly(Glu) in an environment of hydrogen bonding.
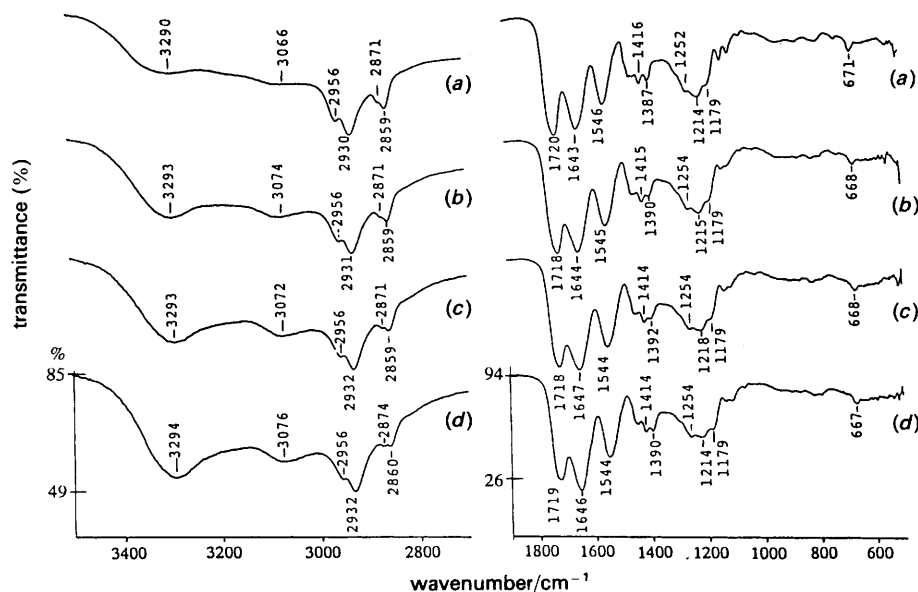
Fig. 1 α-Helical-type IR spectra of octanoyl oligomer films [(a) monomer, (b) dimer, (c) trimer and (d) tetramer] cast onto an NaCl plate at 20 °C and 60% relative humidity

α → β₂-like Transition in α-Helical-type Cast Films

Fig. 2 shows the time dependence of the IR spectrum for the α-helical-type cast film of the octanoyl tetramer at 20 °C and 60% relative humidity (r.h.). The IR bands characteristic of the β_2-type structure[9,10] (marked with an asterisk in Fig. 2) increase in intensity with time, until the whole spectrum takes on the appearance of the octanoyl tetramer sample in the crystalline state, for which lattice spacings characteristic of β_2-type structure were confirmed in the X-ray powder diffraction patterns (footnote f in Table 2). In particular, it should be emphasized that the 792–793 cm⁻¹ band characteristic of the β_2 form appears and increases in intensity as the transition proceeds. Furthermore, the β_2-type structure of the octanoyl tetramer film is also characterised by the C=O stretching band at 1732–1734 cm⁻¹, which closely corresponds to that at 1732 cm⁻¹ for β_2-poly(Glu).[23] The band frequencies are much higher than that usually observed for

the dimeric CO_2H carbonyl frequency (1710–1720 cm⁻¹), because they come from the weak CO_2H-amide group interaction [as schematically shown in Fig. 6(c) later]. This observation reveals that an α → β_2-type transition, similar to that in poly(Glu),[10] occurs in the cast film of the octanoyl tetramer at 20 °C. The IR bands arising from the β_2-type structure are much sharper than those observed for the α-helical type cast films, indicating that the degree of crystallinity or the order of the β_2-type structure is higher than that of the α-type structure in the cast films.

The appearance of a similar transition was followed through the IR spectrum of the α-type cast film of the octanoyl trimer. The IR bands characteristic of a β_2-type structure, which appeared and increased in intensity with the transition, are listed in Table 2 together with those of β_2-type octanoyl trimer, as confirmed by X-ray powder patterns.
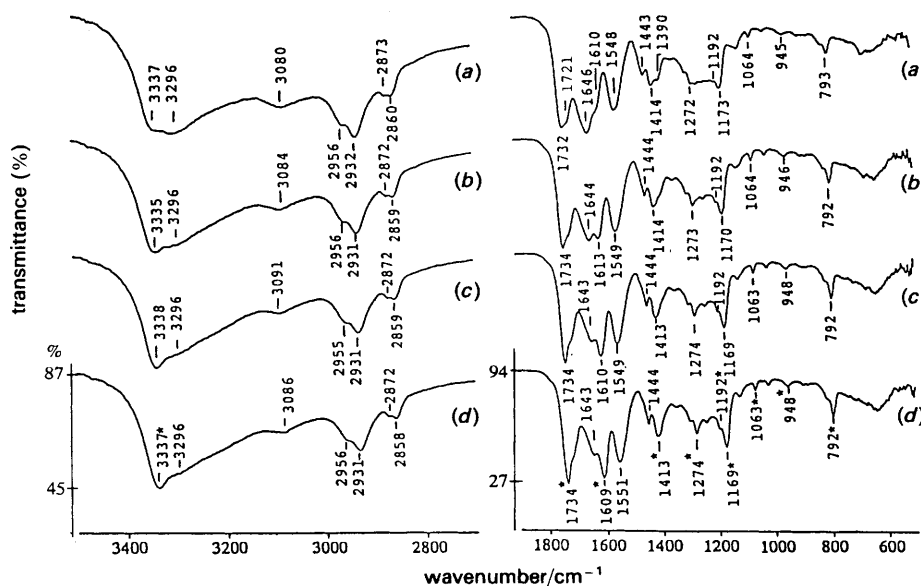
Fig. 2 Time dependence of the IR spectrum for the film of the octanoyl tetramer cast onto an NaCl plate at 20 °C and 60% relative humidity. t/h: (a) 0.17, (b) 1, (c) 3, (d) 12. The bands marked with an asterisk are characteristic of the β_2-type structure.[9,10]

The rate of the $\alpha \rightarrow \beta_2$-type transition for the α-type cast film of the tetramer can easily be determined from the time dependence of the relative absorbance, $A_{1732-1734}/A_{1721-1722}$, of the IR bands from the C=O stretching modes or of that, $A_{1643-1646}/A_{1609-1610}$, from the amide I modes, as shown in Fig. 3A. The transition at 70% r.h. proceeds rapidly compared with that at 60% r.h.
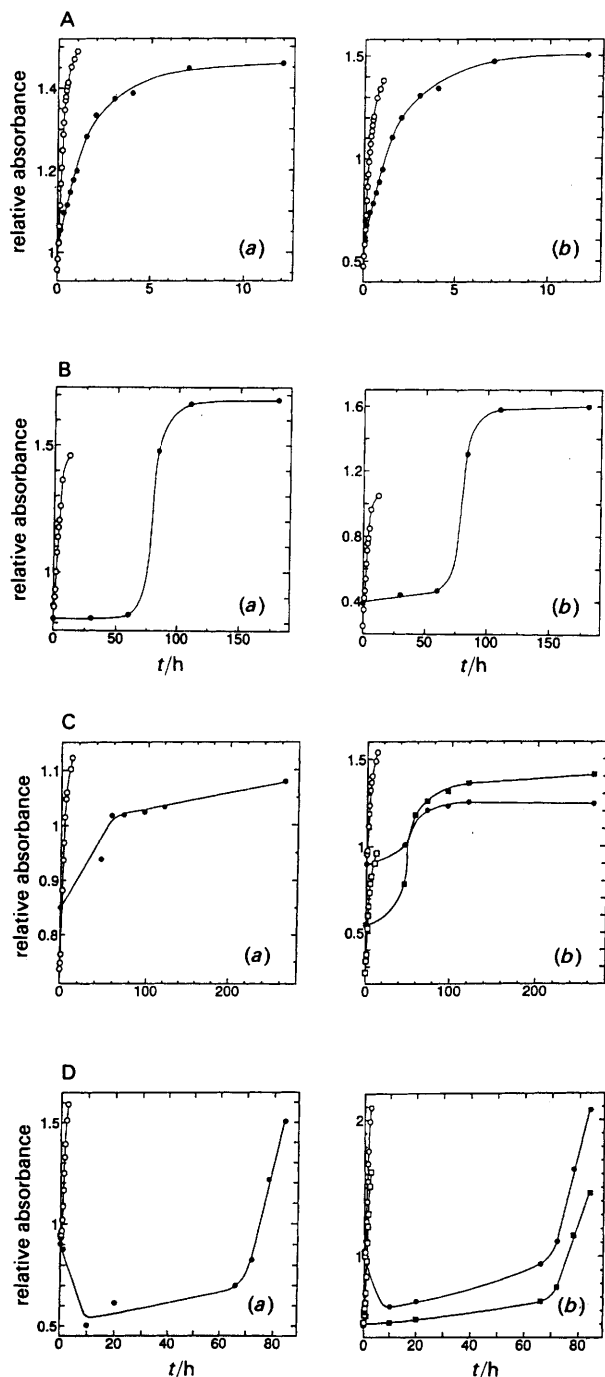

Fig. 3 Time dependence of the relative absorbance of the IR bands in the 1590–1750 cm^{-1} regions. A, Octanoyl tetramer; (a) ●, A_{1734}/A_{1722} at 60% r.h.; ○, A_{1734}/A_{1721} at 70% r.h. (b) A_{1609}/A_{1646} at 60% (●) and 70% (○) r.h. B, Octanoyl trimer; (a) ●, A_{1735}/A_{1718} at 60% r.h.; ○, A_{1735}/A_{1716} at 70% r.h. (b) ●, A_{1604}/A_{1647} at 60% r.h.; ○, A_{1599}/A_{1648} at 70% r.h. C, Octanoyl dimer; (a) ●, A_{1731}/A_{1720} at 60% r.h.; ○, A_{1703}/A_{1718} at 70% r.h. (b) ●, A_{1655}/A_{1644} at 60% r.h.; ○, A_{1652}/A_{1644} at 70% r.h.; ■, A_{1610}/A_{1644} at 60% r.h.; □, A_{1596}/A_{1644} at 70% r.h. D, Octanoyl monomer; (a) ●, A_{1733}/A_{1719} at 60% r.h.; ○, A_{1732}/A_{1719} at 70% r.h. (b) ●, A_{1644}/A_{1630} at 60% r.h.; ○, A_{1643}/A_{1631} at 70% r.h.; ■, A_{1599}/A_{1630} at 60% r.h.; □, A_{1597}/A_{1631} at 70% r.h.

For the case of the octanoyl trimer (Fig. 3B), the A_{1623}/A_{1647} and A_{1735}/A_{1718} ratios at 70% r.h. increase rapidly with time, compared with the A_{1620}/A_{1647} and A_{1735}/A_{1716} ratios at 60% r.h.

These observations imply that the α-helical-type structures of the octanoyl trimer and tetramer in the cast films are further destabilized at higher relative humidity.

In order to study the effect on a C-terminal residue of further destabilization of such an α-helical-type structure at higher relative humidity, a detailed IR investigation was made of the transition for the α-helical-type cast films of the octanoyl monomer and dimer.
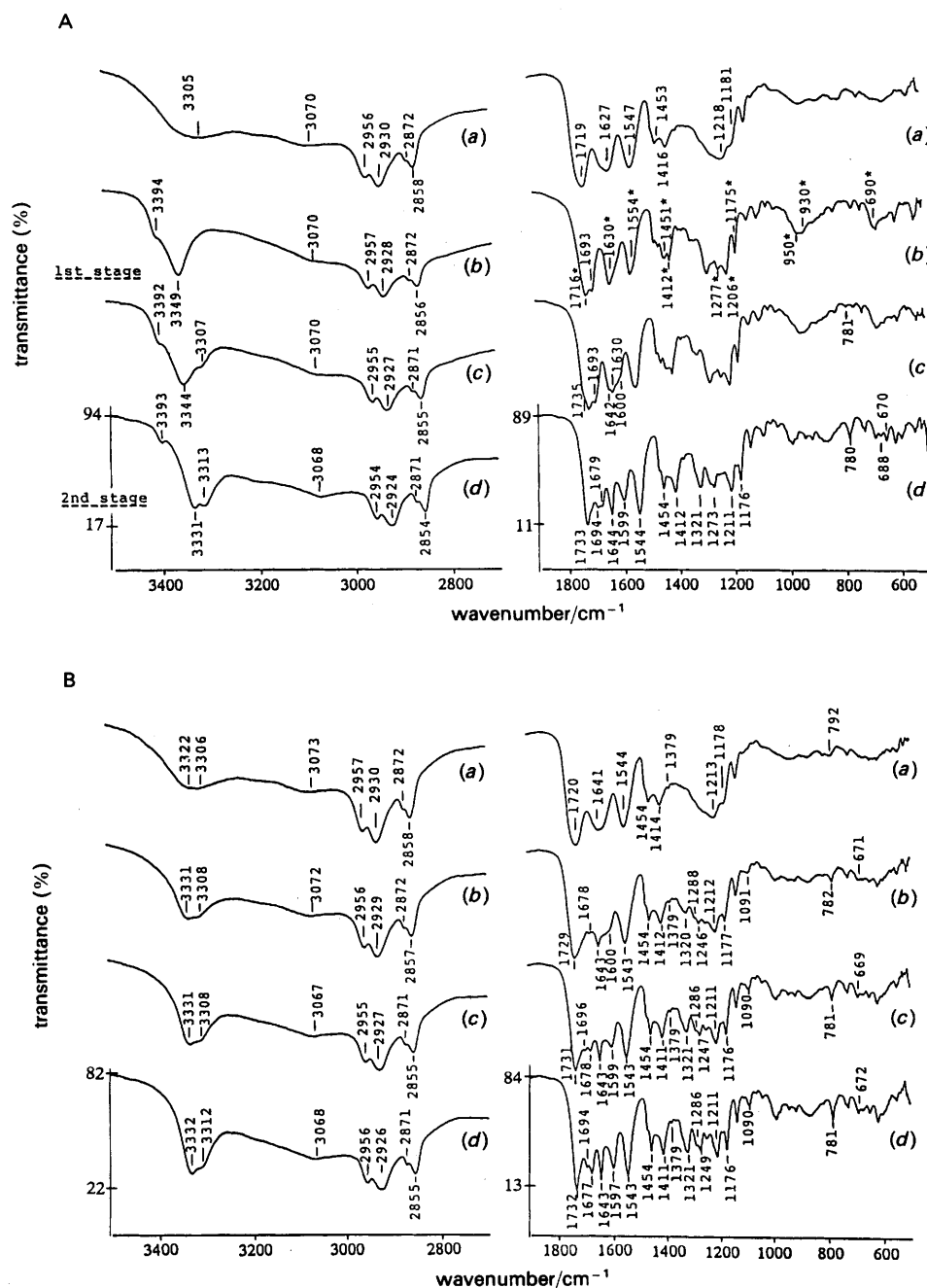
Fig. 4A shows the time dependence of the IR spectrum for the α-helical-type octanoyl monomer cast onto an NaCl plate at 20 °C and 60% r.h. The IR bands characteristic of the β_1-type conformation (marked with an asterisk in Fig. 4A) become predominant as the transition proceeds, until the β_1-type IR spectral feature remains unchanged. The observed bands characteristic of a β_1-type structure are also listed in Table 3 together with those of the longer β_1-type octanoyl oligomers[9] and of β_1-poly(Glu).[10] It should be emphasized that this β_1-type spectral feature of the cast film implies a similarity of the side-chain structure between the monomer cast film and the β_1-type poly(Glu).

After the passage of 20 h, further variation of this IR spectral feature occurs until it again becomes unchanged. The IR spectrum finally obtained can be accounted for by combining the α- and β-type spectra rather than from either of the individual spectra. Thus, the transition of the α-helical-type cast film of the octanoyl monomer occurs in two stages [$\alpha \rightarrow \beta_1 \rightarrow$ mixed type (M)] at 20 °C and 60% r.h. However, at 70% r.h. it was found that the $\alpha \rightarrow$ M transition occurs rapidly and no $\alpha \rightarrow \beta_1$ stage is observed (Fig. 4B).

For the octanoyl monomer cast film, the A_{1733}/A_{1719} and A_{1644}/A_{1630} ratios plotted as a function of time at two different relative humidities (60 and 70%) are shown in Fig. 3D. The time dependence of these ratios indicates that the transition at 70% r.h. proceeds rapidly compared with that at 60% r.h.

Fig. 5 shows the time dependence of the IR spectrum for the α-helical-type cast film of the octanoyl dimer. The $\alpha \rightarrow \beta_2$-type transition occurs at 60% r.h. The bands characteristic of a β_2-structure are marked with an asterisk. In the IR spectrum obtained upon transition at 70% r.h., the 1387–1392 cm^{-1} bands characteristic of α-helical poly(Glu)[23] are not found. However, the IR bands at 1183, 1214, 1279, 1415, 1451, 1544 and 1652 cm^{-1} correspond well to those at 1181, 1212, 1283, 1415, 1451, 1550 and 1653 cm^{-1} for α-helical poly(Glu), respectively. Furthermore, the very weak IR bands at 660 cm^{-1} may correspond to the amide V band at 670 cm^{-1} for α-poly(Glu).[23] Therefore, the IR spectrum of the octanoyl dimer film obtained at 70% r.h. is similar to that of an α-type structure. Since in the normal-mode calculations for α-helical poly(Glu)[23] the 1388 cm^{-1} band is assigned to the wagging modes [potential-energy distribution (PED) 36%] of the side-chain CH$_2$ groups coupled with the H$^{\alpha}$ bending mode (PED 22%) and C$^{\beta}$—C$^{\gamma}$ stretching mode (PED 13%), the 1387–1392 cm^{-1} band may be associated with the side-chain conformation. Accordingly, the absence of the 1387–1392 cm^{-1} bands in the IR spectrum of the octanoyl dimer film obtained at 70% r.h. may imply a local conformational change of the side-chain accompanying higher crystallinity.

When the transition of the octanoyl dimer film occurs at 70% r.h., the IR bands arising from the C=O stretching modes of the side-chain CO$_2$H groups are found to split with time into two bands at 1703–1715 and 1736–1738 cm^{-1}. In particular, the 1715 cm^{-1} band shifts to 1703 cm^{-1}, indicat-

Fig. 4 Time dependence of the IR spectrum for the film of the octanoyl monomer cast onto an NaCl plate at 20 °C. A, 60% r.h.: t/h: (a) 0, (b) 10, (c) 66, (d) 84. B, 70% r.h.: t/h: (a) 0.5, (b) 0.83, (c) 1.17, (d) 2. The bands characteristic of β_1-structure are marked with an asterisk.

ing that the dimeric hydrogen bonds formed between pairs of side-chain carboxyl groups become stronger with higher crystallinity. The appearance of the 1736–1738 cm^{-1} bands implies that the carboxyl groups partially participate in the weakly hydrogen-bonded CO_2H system.

The A_{1731}/A_{1720} and A_{1655}/A_{1644} ratios for the transition at 60% r.h. and the A_{1703}/A_{1738} and A_{1652}/A_{1644} ratios at 70% r.h. are plotted as a function of time in Fig. 3C. It is also evident that the transition at 70% r.h. proceeds more rapidly than that at 60% r.h.

Thus, we may assume that the α-helical-type structure for the cast films of the octanoyl monomer and dimer is further destabilized at higher relative humidity. The following discussion is concentrated on the origin of this further destabilization.

CO_2^- Group Effect on the Transition

For the α-helical-type cast films of the octanoyl monomer, dimer and trimer, as the transition progresses the IR bands at 1590–1602 cm^{-1} appear in common and increase in intensity (Fig. 4 and 5 and Table 2). Assignment of these bands plays a critical role in understanding the mechanism of the transition promoted at the higher relative humidity.

For the cast film of the octanoyl monomer, when we assign the 1599–1600 cm^{-1} bands to either the amide I or the amide II mode, the reason for appearance of the two amide I bands at 1599–1600 and 1643 cm^{-1} or the two amide II bands at 1544 and 1599–1600 cm^{-1} must be explained. However, it is very difficult to explain the magnitude (43–44 or 55–56 cm^{-1}) of the band splitting by the transition dipole–dipole (TDD) interaction mechanism,[25-27] which has been attrib-
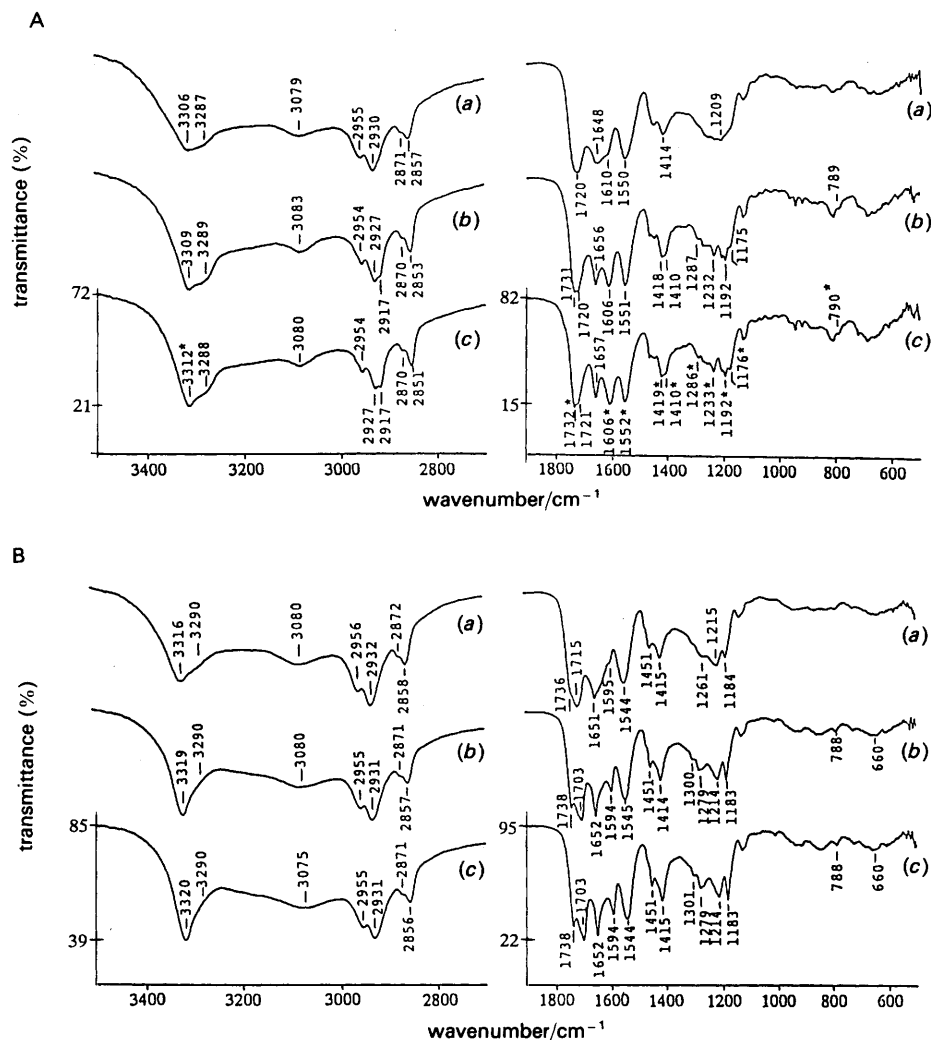
Fig. 5 Time dependence of the IR spectrum for the film of the octanoyl dimer cast onto an NaCl plate at 20 °C at two different relative humidities [60% (A) and 70% (B)]: A, (a) 46 h; (b) 58 h and (c) 264 h; B, (a) 2 h; (b) 6 h and (c) 12 h. The bands characteristic of a β_2-type structure are marked with an asterisk in A.

uted to the splitting of the amide I and II bands, depending on the secondary structure of the polypeptide chains and their packing.[25–27] The TDD interaction mechanism is most effective between adjacent intramolecular peptide groups.[27] Accordingly, in the case of the octanoyl monomer the TDD interaction mechanism may not be so effective, even if tight packing of the octanoyl chains occurs, since there is only one peptide group in a monomer molecule. Thus, assignment of the 1599–1600 cm^{-1} bands to either the amide I or amide II modes is unreasonable. We suggest that these bands should be assigned to the asymmetric stretching mode of a C-terminal α-CO$_2^-$ group rather than to the amide I or amide II mode.

For the IR spectra of sodium salts of the octanoyl oligomers ($N = 1–3$), we have investigated the bands characteristic of the CO$_2^-$ group and these are listed in Table 4. The band at 1568–1572 cm^{-1} increases in intensity with the number of residues, while the 1589–1600 cm^{-1} band decreases in intensity with the number of residues and appears only as a very weak shoulder in the IR spectrum of the octanoyl trimer salt. Therefore, the former band comes from the γ-CO$_2^-$ group and the latter one from the α-CO$_2^-$ group. The IR bands arising from the CO$_2^-$ scissoring mode are observed at 786 and 847 cm^{-1} for the monomer salt, at 793, 840 and 860 cm^{-1} for the dimer salt and at 787 and 840–860 cm^{-1} for the trimer salt. The band at 786–793 cm^{-1} decreases in intensity with

increasing number of residues. Therefore, these bands may be assigned to the scissoring mode of an α-CO$_2^-$ group.

For the α-type cast films of very simple octanoyl oligomers ($N = 1–3$), as the transition proceeds at 70% r.h., the band at 1590–1600 cm^{-1} arising from the α-CO$_2^-$ asymmetric stretching mode appears in common and increases in intensity (Fig. 4 and 5 and Table 4).

For the IR spectrum of the octanoyl monomer film, the 1597 cm^{-1} band arising from the asymmetric stretching mode of an α-CO$_2^-$ group increases in intensity as the transition progresses. The 1411 cm^{-1} band arises from an overlap of the symmetric stretching mode of an α-CO$_2^-$ group and the CH$_2$ scissoring mode. The 781 cm^{-1} band coming from the α-CO$_2^-$ scissoring mode also increases in intensity as the transition progresses. As the transition proceeds at 60% r.h., the IR bands (1599–1600 and 780–781 cm^{-1}) characteristic of an α-CO$_2^-$ group are also observed in the $\beta_1 \to$ M stage and increase in intensity.

For the cast films of the octanoyl dimer and trimer, at 70% r.h. the bands at 1597–1599 and 788–790 cm^{-1}, characteristic of an α-CO$_2^-$ group appear and increase in intensity as the transition proceeds (Fig. 5 and Table 2). At 60% r.h., no bands at 1590–1600 cm^{-1} are observed. These bands probably overlap with the amide I bands observed at 1606–1610 cm^{-1}.

The IR spectra and band assignment for glutamic acid and

Table 4 CO_2^- characteristic IR band frequencies $(cm^{-1})^a$ for octanoyl oligomer cast films $(N = 1-3)$ and octanoyl oligomer sodium salts $(N = 1-3)$

	$v_{as}(CO_2^-)^b$	$v_s(CO_2^-)^b$	$S_{sic}(CO_2^-)^b$	$R_{rock}(CO_2^-)^b$
monomer cast film	1597 s	1411 m^c	868 b, w, 781 w^c	647 w, 617 w
dimer cast film	1594 s	1415 m^c	846 b, w, 785 vw^c	660 vw
trimer cast film	1598 sh	1412 m^c	792 w^c	
monomer Na-salt	1589 vs, 1571 sh	1418 s	847 m, 786 m	658 vw, 603 w
dimer Na-salt	1600 vs, 1568 s	1414 s	860 m, 840 m, 793 w	667 m, 619 w
trimer Na-salt	1572 vs	1406 s	840–860 vb, w, 787 vw	662 w, 613 w, 602 w

^{a} s, strong; m, medium; w, weak; v, very; sh, shoulder; b, broad. For the cast films the IR band frequencies measured at relative humidity 70% were listed. ^{b} $v_{as}(CO_2^-)$: asymmetric stretching mode, $v_s(CO_2^-)$: symmetric stretching mode, $S_{sic}(CO_2^-)$: scissoring mode and R_{rock}: rocking mode. ^{c} The 1411–1415 cm^{-1} bands overlap with the CH_2 scissoring modes and the 781–792 cm^{-1} bands with the CH_2 rocking modes.

its related compounds, which have already been reported by Takenishi,[28-30] strongly support the present assignment for the IR bands characteristic of an α-CO_2^- group.

From the time dependence of the IR spectrum of the octanoyl monomer cast film, the ratio of absorbance of the 1599 cm^{-1} band to that of the 1630 cm^{-1} band may be useful as a measure of the ionization rate of an α-CO_2H group. The $[A_{1599}]/[A_{1630}]$ ratios are plotted as a function of time at different relative humidities (60 and 70%) in Fig. 3D. The $[A_{1599}]/[A_{1630}]$ ratio at 70% r.h. increases rapidly compared with that at 60% r.h. In the case of the octanoyl dimer and trimer (Fig. 3B and C), it is also evident that the $[A_{1595-1602}]/[A_{1643-1644}]$ ratio at 70% r.h. increases very rapidly compared with the $[A_{1604-1610}]/[A_{1644-1645}]$ ratio at 60% r.h. These results imply that ionization of an α-CO_2H in the cast films is promoted at higher relative humidity. In other words, an α-helical-type structure in the cast films of octanoyl oligomers is destabilized by an α-CO_2^- group.

By using circular dichroism, Kim and Baldwin[3] found that for the isolated C-terminal peptide (residues 1–13 of ribonuclease A) a terminal α-CO_2^- group destabilizes the helical structure. Conversely, for very short N-acylglycine oligomers $(N = 3-5)$, Okabayashi et al.[6,7] reported that a terminal α-CO_2^- group stabilizes a helical structure similar to that of polyglycine II. Therefore, the α-CO_2^- group effect may depend on the nature of the amino acid residues.

Packing Variation of N-Octanoyl Chains and CH Stretching Modes

For the α-helical octanoyl monomer, the $\alpha \rightarrow \beta_1 \rightarrow M$ transition at 60% r.h. shifts the bands at 2859–2860 and 2930–2932 cm^{-1} to 2854 and 2924 cm^{-1}, respectively, while the frequency of bands at 2871–2874 and 2956 cm^{-1} remains almost unchanged as the transition proceeds (Fig. 4 and Table 2). When the transition of the α-type cast films of the octanoyl dimer and trimer occur at 60% r.h., the 2859 cm^{-1} band shifts to 2851–2852 cm^{-1} and the bands at 2931–2932 cm^{-1} split into two bands (2917–2918 and 2927–2929 cm^{-1}) (Fig. 4 and 5 and Table 2). Furthermore, the band at 2851–2859 cm^{-1} tends to increase in intensity with the progress of the transition.

It has already been shown that the CH stretching bands of an n-alkyl chain are very sensitive to change in frequency and bandwidth with variation of the chain-packing and ordering.[31,32] For example, for barium ethyloctyl phosphate[33] in the solid state the CH stretching bands of the n-octyl chain were observed at 2850, 2869, 2891, 2918, 2951 and 2973 cm^{-1}, but the bands at 2850 and 2918 cm^{-1} were shifted to 2857 and 2927 cm^{-1}, respectively, and became broader in aqueous solution and at high temperature, reflecting a reduction in the intermolecular vibrational coupling due to the packing variation and the decreased ordering of the n-octyl chain.[31,32]

Thus, the shifting and splitting of the CH stretching bands observed for very simple octanoyl oligomers at 60% r.h. could be due to the packing variation of the octanoyl chains. The new bands at 2917–2918 cm^{-1} may be assigned to the CH stretching band of the octanoyl group. These observations reveal that the transition for the α-type cast films of octanoyl oligomers $(N = 1-3)$ results in variation of the packing state between octanoyl chains. Thus, we may assume that in the β_1- or β_2-type cast films of octanoyl oligomers $(N = 1-3)$ the octanoyl chains are in a more densely packed state than those in the α-type films.

In the α-helical-type cast films of the octanoyl monomer, dimer and trimer, the degree of crystallinity or of order may be diminished or absent, as mentioned above. Therefore, we may assume that the octanoyl chains are dispersed in the cast film and are in an unstable state. The hydrophobic interactions between the octanoyl chains, as well as those between the side chains, probably play an important role in formation of higher ordered arrangements of chains as the transition proceeds.

For the octanoyl monomer cast film, no splitting of the 2930–2932 cm^{-1} band is observed at 70% r.h. However, this band becomes broader with the progress of the transition (Fig. 4B), implying that packing variation does occur. For the dimer and trimer cast films, any shifting of the 2958 cm^{-1} band is very small and no splitting of the 2930–2932 cm^{-1} band occurs, indicating that variation in the packing state of the octanoyl chains is small at higher relative humidity. Under these conditions, the predominant cause of the conformational change of the peptide groups in the cast films of the octanoyl dimer and trimer comes from the α-CO_2^- group effect, rather than from the hydrophobic interaction. Consequently, tight packing of the octanoyl chains is blocked.

NH Stretching Modes

For the α-helical-type cast films of octanoyl oligomers the transition at 60% r.h. brings about a drastic variation in the NH stretching modes (Fig. 1, 2, 4 and 5). For the octanoyl monomer, the NH stretching band shifts to higher frequency and splits into two bands at 3349 and 3394 cm^{-1} as the transition proceeds (Fig. 4A). We may therefore assume that the NH hydrogen-bonding networks are released with the progress of an $\alpha \rightarrow \beta_1$ stage and that the weaker NH hydrogen-bonding system is stabilized, compared with that in the α-helical-type cast films. During the second stage $(\beta_1 \rightarrow M)$, a new band at 3307–3313 cm^{-1} appears in addition to the bands at 3349 and 3394 cm^{-1}, and increases in intensity with progression of the transition. At the final stage of transition, the NH hydrogen-bonding networks consist of three different bonding modes. The two weak NH hydrogen-bonding systems, corresponding to the 3313 and 3331 cm^{-1} bands, are predominantly stabilized and the very weak or

almost free NH hydrogen-bonding system is only slightly formed.

At 70% r.h., the 3394 cm^{-1} band disappears throughout the transition process (Fig. 4B), and the spectral feature in the NH stretching region rapidly comes close to that observed at 60% r.h.

The transition is also reflected in the NH stretching modes for the cast films of the octanoyl dimer, trimer and tetramer, as seen in Fig. 2–5 and Table 2. Spectral variation (both in band frequency and intensity) in the NH stretching region, caused by the transition, depends strongly on the number of residues and relative humidity. In particular, for the cast film of the octanoyl trimer at 70% r.h., the spectral features in the NH stretching mode are very similar to those for the cast film of the octanoyl tetramer.

As mentioned above, for the cast films of the octanoyl oligomers ($N = 1–3$) the transition at 60% r.h. results in a tightly packed state of octanoyl chains. This process must induce marked variation in intra- and inter-molecular hydrogen-bonding networks formed by the NH groups, which are reflected directly in the spectral features in the NH stretching region.

Conclusion

From IR spectroscopic evidence we may conclude that even the octanoyl monomer and dimer, as well as the octanoyl trimer and tetramer, take up an α-helical-type structure in the films cast onto an NaCl plate. This observation indicates that the hydrogen-bonding networks formed by the α-, γ-carboxyl and peptide groups may be very similar to α-helical poly(Glu)

in their environment. Furthermore, we may assume that the degree of crystallinity or of higher order is small or lacking in these α-helical-type cast films.

Fig. 6(a) shows a schematical model for an α-helical-type structure in the cast film of an octanoyl trimer. In this model, in which the three glutamic acid residues take up an α-helix, hydrogen bonding between the side-chain carboxyl groups of the nearest-neighbouring molecules is emphasized. Probably, however, the C=O and NH groups of a peptide group will also take part in the hydrogen-bonding systems. Octanoyl chains may be in a loosely packed state rather than in a densely packed one. This model may also apply to the α-type structure of the octanoyl monomer and dimer.

For the α-type cast films of the octanoyl oligomers ($N = 1–4$), the IR spectra provide evidence that a transition similar to the $\alpha \to \beta_1$ or $\alpha \to \beta_2$ transition of poly(Glu) occurs with time and is promoted at higher relative humidity. For the cast films of the octanoyl monomer, dimer and trimer, as the transition proceeds at 70% r.h., the IR bands at 1591–1599 cm^{-1} (arising from the asymmetric stretching modes of an α-CO$_2^-$ group) appear in common and rapidly increase in intensity.

However, when the transition for these cast films occurs at 60% r.h., the band arising from the α-CO$_2^-$ asymmetric stretching modes is observed at 1599 cm^{-1} for the monomer and at 1604–1610 cm^{-1} (overlapping with the amide I modes) for the dimer and trimer, and these bands slowly increase in intensity compared with the transition at 70% r.h.

This observation suggests that, in these α-type cast films, dissociation of an α-CO$_2$H group is promoted at a higher relative humidity and that the α-helical-type structure is destabilized by the singly charged α-CO$_2^-$ group.
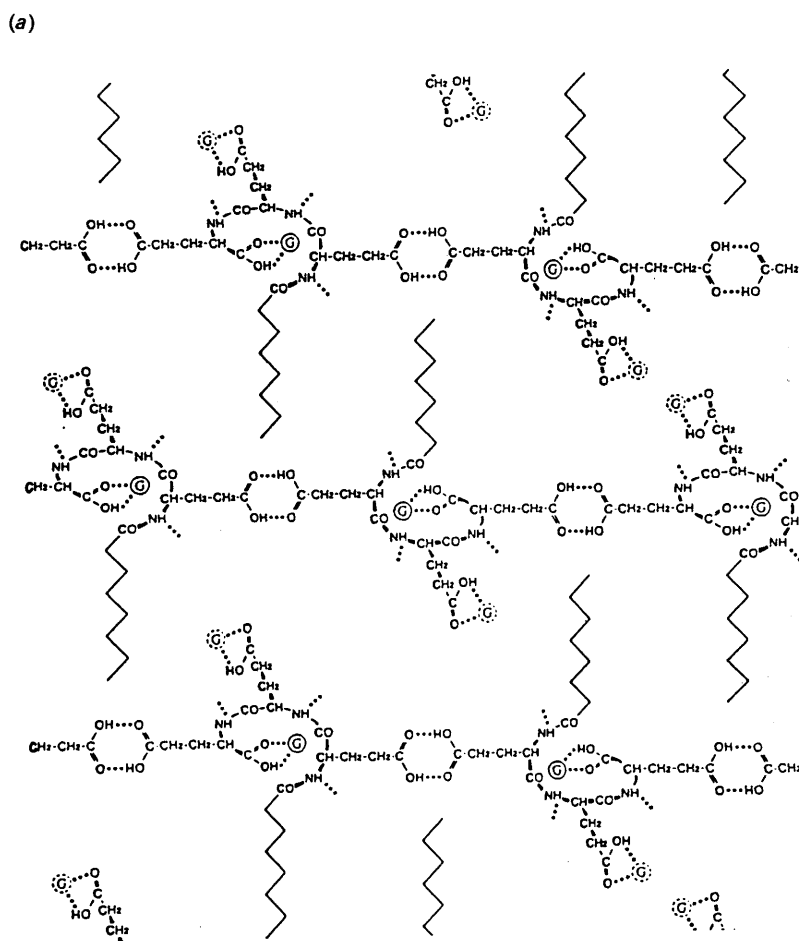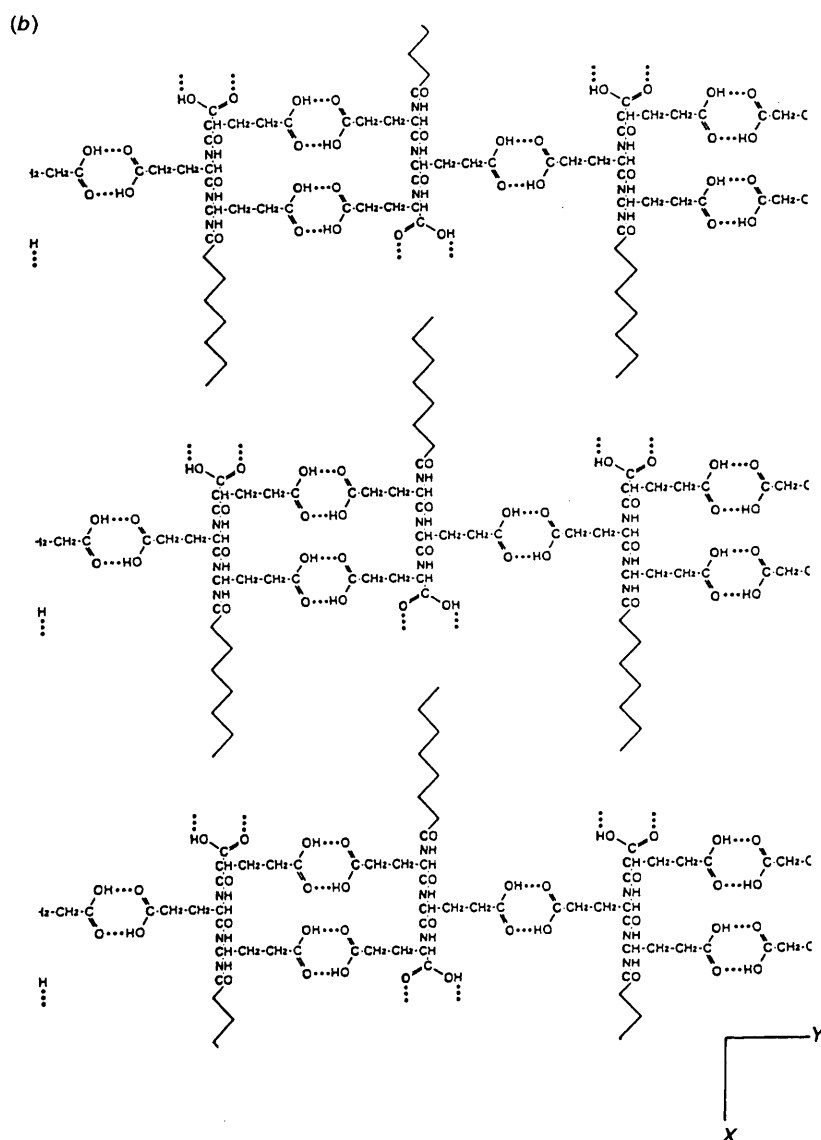
(a)

Fig. 6 (a)

(b)

Fig. 6 (b)

The IR spectra in the CH stretching region provide evidence that variation in the packing state for octanoyl chains occurs and that the octanoyl chains are more densely packed at the final stage of transition.

In order to explain the transition for these cast films, it may be assumed that the transition process involves packing variation of the octanoyl chains and structural variation in the hydrogen-bonding networks formed by the side chains. The two structural models, based on the β_1- and β_2-structures of poly(Glu),[10] and the α-helical-type structure, are shown schematically in Fig. 6 for the representative octanoyl trimer case. For one of the two models [Fig. 6(b)], the planes of the carboxyl groups of the side chains lie parallel to the chain axis and hydrogen bonds are formed between pairs of carboxyl groups, belonging to different neighbouring sheets, (β_1-type model). In another model [Fig. 6(c)], the side-chain CO_2H groups lie in a plane normal to the chain axis and this arrangement enables the side chains to interpenetrate deeply within each other (β_2-type model).

In the monomer cast film at 60% r.h., the hydrophobic interactions between the octanoyl chains or the glutamic acid side chains, may allow the $\alpha \rightarrow \beta_1$ type transition (corresponding to that from the α-type model to the β_2-type model) to occur at the first stage of this transition. Structural changes in the hydrogen-bonding networks formed by the side-chain CO_2H groups are dominant at this stage. However, slow ionization of an α-CO_2H group causes further transition ($\beta_1 \rightarrow M$) of the cast film [Fig. 3(D)]. In the final state (M state) the side-chain CO_2H groups may interpenetrate deeply, as in the β_2-type model [Fig. 6(c)].

For the cast films of the octanoyl dimer and trimer, no spectral variation corresponding to the $\alpha \rightarrow \beta_1$ stage was observed, suggesting that the transition from the α-type model to the β_2-type model occurs rapidly. This process may also cause packing variation of the octanoyl chains.

(c)

Fig. 6 (c)
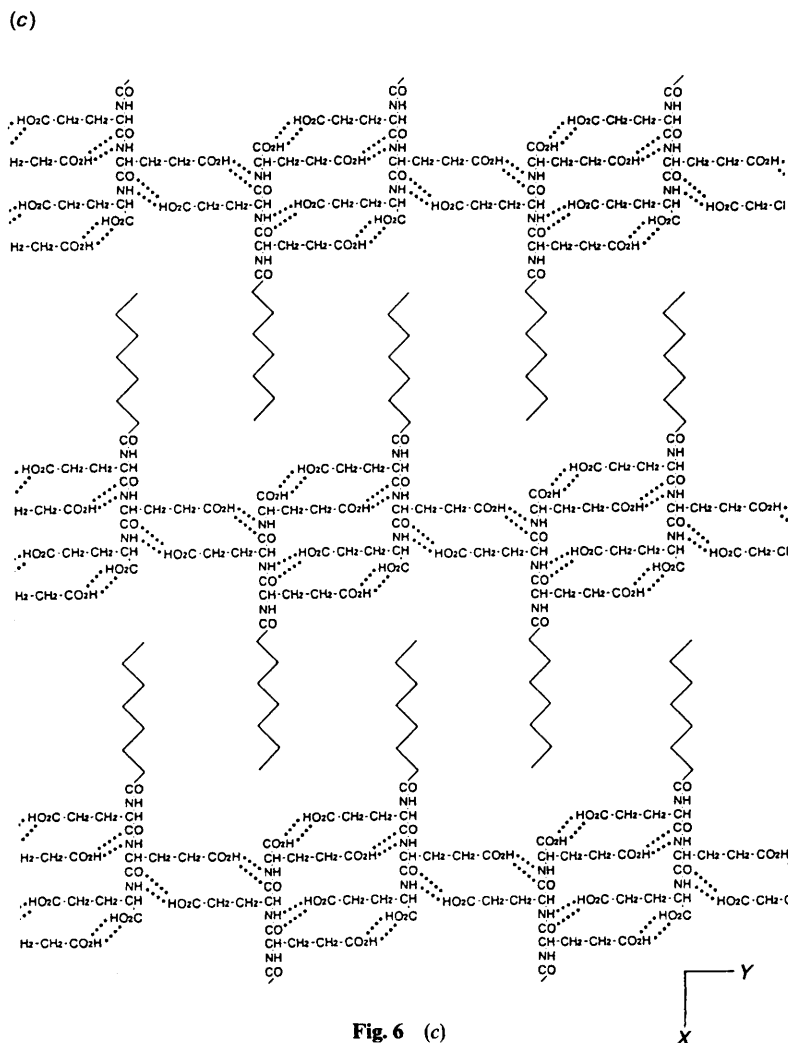
Fig. 6 α-Helical type (a), β_1-type (b) and β_2-type (c) structural models for the cast film of the octanoyl trimer. The dotted lines represent hydrogen bonding. In the model (a), a G circled by a solid line denotes a glutamic acid residue in the upper position and while a G circled by a dotted line denotes a glutamic acid at the lower position. The three residues of glutamic acid are in the same positions as the three residues in the α-helical poly(Glu). All the α,γ-CO$_2$H and peptide groups participate in the hydrogen-bonding network. In the β_1-type model (b), the planes of the carboxyl groups of the side chains lie parallel to the chain axis, but in the β_2-type model (c) the carboxyl groups lie in a plane normal to the chain axis. In the two β-form models, the β-sheets are expanded in the Y–Z plane.

References

1 G. E. Schulz and R. H. Shirmer, *Principles of Protein Structure*, Springer, New York, 1979.
2 A. Bierzynski, P. S. Kim and R. L. Baldwin, *Proc. Natl. Acad. Sci. USA*, 1982, **79**, 2470.
3 P. S. Kim and R. L. Baldwin, *Nature (London)*, 1984, **307**, 329.
4 K. R. Shoemaker, P. S. Kim, D. N. Brems, S. Marqusee, E. J. York, I. M. Chaiken, J. M. Stewart and R. L. Baldwin, *Proc. Natl. Acad. Sci. USA*, 1985, **82**, 2349.
5 D. E. Blagdon and M. Goodman, *Biopolymers*, 1975, **14**, 241.
6 H. Okabayashi, K. Ohshima, H. Etori, K. Taga, T. Yoshida and E. Nishio, *J. Phys. Chem.*, 1989, **93**, 6638.
7 H. Okabayashi, K. Ohshima, H. Etori, R. Debnath, K. Taga and T. Yoshida, *J. Chem. Soc., Faraday Trans.*, 1990, **86**, 1561.
8 T. Uehara, Y. Yamada, H. Okabayashi, K. Taga, T. Yoshida and H. Kojima, to be published.
9 T. Uehara, H. Okabayashi, K. Taga, T. Yoshida and H. Kojima, *J. Chem. Soc., Faraday Trans.*, 1992, **88**, 3451.
10 K. Itoh, B. M. Foxman and G. D. Fasman, *Biopolymers*, 1976, **15**, 419.
11 H. D. Keith, G. Giannoni and F. J. Padden, *Biopolymers*, 1969, **7**, 775.
12 H. D. Keith, F. J. Jr. Padden and G. Giannoni, *J. Mol. Biol.*, 1969, **43**, 423.
13 G. D. Fasman, K. Itoh, C. S. Liu and R. C. Lord, *Biopolymers*, 1978, **17**, 1729.
14 P. K. Sengupta and S. Krimm, *Biopolymers*, 1985, **24**, 1479.
15 E. J. Ambrose and A. Elliott, *Proc. R. Soc. London, Ser. A*, 1951, **205**, 47.
16 T. Miyazawa and E. R. Blout, *J. Am. Chem. Soc.*, 1961, **83**, 712.
17 K. Itoh and T. Shimanouchi, *Biopolymers*, 1970, **9**, 383.
18 E. M. Ambrose, *J. Chem. Soc.*, 1950, 3239.
19 E. R. Blout and M. Idelson, *J. Am. Chem. Soc.*, 1956, **78**, 497.
20 H. Lenormant, A. Baudras and E. R. Blout, *J. Am. Chem. Soc.*, 1958, **80**, 6191.
21 J. L. Koenig and B. Frushour, *Biopolymers*, 1972, **11**, 1871.
22 T. Miyazawa and E. R. Blout, *J. Am. Chem. Soc.*, 1961, **83**, 712.
23 P. K. Sengupta and S. Krimm, *Biopolymers*, 1985, **24**, 1479.
24 G. D. Fasman, in *Poly-α-Amino Acids*, ed. G. D. Fasman, Marcel Dekker, New York, 1967, p. 499.
25 Y. Abe and S. Krimm, *Biopolymers*, 1972, **11**, 1817.
26 S. Krimm and Y. Abe, *Proc. Natl. Acad. Sci. USA*, 1972, **69**, 2788.
27 Yu. N. Chirgadze and N. A. Nevskaya, *Dokl. Acad. Nauk SSSR*, 1973, **208**, 447.
28 T. Takenishi, *Nippon Kagaku Zasshi*, 1960, **81**, 1496.
29 T. Takenishi, *Nippon Kagaku Zasshi*, 1961, **82**, 16.
30 T. Takenishi, *Nippon Kagaku Zasshi*, 1961, **82**, 806.
31 T. Kawai, J. Umemura, T. Takenaka, M. Kodama and S. Seki, *J. Colloid Interface Sci.*, 1985, **103**, 56.
32 H. H. Mantsch, *J. Mol. Struct.*, 1984, **113**, 201.
33 K. Miyagai, K. Taga, T. Yoshida, H. Okabayashi and E. Nishio, *Colloid Polym. Sci.*, 1991, **269**, 153.